A Novel Pathway of Protein Haptenation by β-Lactams

Raúl Pérez-Ruíz,[a] Emilio Lence,[b] Inmaculada Andreu,[c] Daniel Limones-Herrero,[a] Concepción González-Bello,[b] Miguel A. Miranda*[a] and M. Consuelo Jiménez*[a]

Abstract: The covalent binding of β-lactams to proteins upon photochemical activation has been demonstrated using an integrated approach that combines photochemical, proteomic and computational studies, selecting human serum albumin (HSA) as target protein and ezetimibe (**1**) as probe. The results have revealed a novel protein haptenation pathway by this family of drugs that is alternative to the known nucleophilic ring opening of β-lactams by the free amino group of lysine residues. Thus, photochemical ring splitting of the β-lactam ring following a formal retro-Staudinger reaction gives a highly reactive ketene intermediate that is trapped by the neighbouring lysine residues, leading to an amide adduct. For the investigated **1**/HSA system, covalent modification of Lys414 and Lys525 residues, which are located in sub-domains IIIA and IIIB, respectively, occurs. The observed photobinding may constitute the key step in the sequence of events leading to photoallergy. Docking and Molecular Dynamics simulation studies provide an insight into the molecular basis of the selectivity of **1** for these HSA sub-domains and the covalent modification mechanism. The computational studies also reveal a positive cooperative binding of sub-domain IIIB that explains the experimentally observed modification of Lys414, which is located in a hardly accessible pocket (sub-domain IIIA).

Introduction

Drugs containing the β-lactam ring (azetidinones) are the first choice for the treatment of a broad range of bacterial diseases. That is the case of the widely prescribed β-lactam antiobiotics, such as penicillins, cephalosporins and monobactams, which have saved millions of lives and whose discovery has been one of the most important achievements in the history of Medicine (Chart 1). Also relevant are β-lactamase inhibitors, such as clavams and carbapenems, which are used to block the most prevalent cause of antibiotic resistance in bacteria, thus the enzymatic inactivation of drugs by β-lactamases. In 2010, the international consumption of β-lactams made up 65% of the global antibiotics market.[1]

Currently marketed β-lactams are responsible for inducing a variety of adverse reactions; allergy is probably the most important and can be manifested as pruritus, erythema, urticaria, dermatitis, fever, asthma or even anaphylactic shock.[2] The most frequently reported allergy problems are due to penicillins, with up to 10% of patients exhibiting hypersensitivity to these drugs, followed by cephalosphorins.[3] Less prevalent but also significant are the allergic processes due to carbapenems, clavams and monobactams (Chart 1).[4],[5] These allergic diseases are due to the interaction of β-lactam drugs with the immune system that has been mainly explained by the hapten hypothesis. It is based on the observation that small organic molecules do not induce an immune response unless they are covalently bound to a protein.[6]

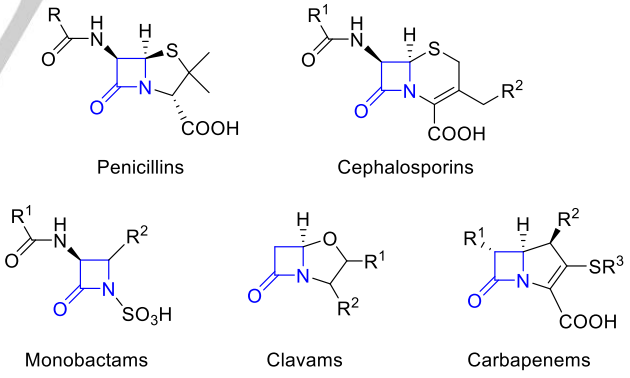

Chart 1. Chemical structures of some families of β-lactam antibiotics and inhibitors of antibiotic resistance that contain the β-lactam moiety.

Actually, β-lactams have been used to prove such hypothesis, based on the high reactivity associated with the strained four membered ring that facilitates covalent binding to proteins through a nucleophilic attack by the amino groups.[7] In this context, the most widely studied β-lactam is benzylpenicillin, which is considered a reference model.[8] Opening of its four-membered ring by a protein amino group leads to a benzylpenicilloyl adduct through formation of an amide linkage. Similar results have been reported for amoxicillin, the most

[a] Dr. R. Pérez-Ruiz, Dr. D. Limones-Herrero, Prof. M. A. Miranda, Prof. M. C. Jiménez
Departamento de Química/Instituto de Tecnología Química UPV-CSIC
Universitat Politècnica de Valencia,
Camino de Vera s/n
46071 Valencia, Spain
E-mail: mmiranda@qim.upv.es; mcjimene@qim.upv.es
[b] Dr. E. Lence, Prof. C. González-Bello
Centro Singular de Investigación en Química Biolóxica e Materiais Moleculares (CIQUS) and Departamento de Química Orgánica,
Universidade de Santiago de Compostela,
calle Jenaro de la Fuente s/n,
15782 Santiago de Compostela, Spain
[b] Dr. I. Andreu
Instituto de Investigación Sanitaria La Fe,
Hospital Universitari i Politècnic La Fe,
Avenida de Fernando Abril Martorell 106,
46026 Valencia, Spain

Supporting information for this article is given via a link at the end of the document.

prescribed member of the family.[9] The main structural difference between cephalosporins and penicillins is the nature of the ring to which the β-lactam is fused, a 6-member dihydrothiazine in the former and a 5-member thiazolidine in the latter. This feature modifies the electrophilic properties of the carbonyl group and, therefore, its potential to react with proteins.[10] Comparatively, little is known about drugs containing a monocyclic β-lactam moiety, although the available chemical data suggest that they should be much less reactive towards amines and hence more reluctant to undergo covalent attachment to proteins. For the above reasons, the covalent binding of β-lactams to carrier proteins has been intensively investigated, paying attention to detection and identification of the products.

Human serum albumin (HSA) is a carrier protein often employed for model studies. It is the most abundant protein in human plasma, complexing a wide variety of endogenous as well as exogenous ligands.[11] Thus, HSA has been considered as the main target protein in the haptenation by penicillins, and a number of studies have focused on characterization of penicilloyl-HSA adducts. Although the factors that determine which amino acids become modified by β-lactams are not fully established, lysine residues are clearly more reactive.[12]

With this background, it appears relevant to explore whether photochemical activation of β-lactams may enhance covalent binding to proteins, a process that constitutes the key step in the sequence of events leading to photoallergy. This is an important issue, and the public health problem associated with photobiological risk has been recognized by the major regulatory entities (EMA, FDA, etc.), who have issued a set of guidelines for compulsory photosafety testing of new active compounds.

In the present work, the photoinduced binding of β-lactam to proteins has been investigated using an integrated approach that combines photochemical, proteomic and docking and Molecular Dynamics (MD) simulation studies, selecting HSA as target protein and ezetimibe (**1**, Chart 2) as probe. This recently marketed drug contains a monocyclic β-lactam core and its main function is to decrease the plasma cholesterol levels, acting as selective absorption inhibitor in the small intestine and reducing in this way the amount of cholesterol normally available to liver cells. This mode of action is complementary to that of statins, and is recommended as a second line treatment.[13] Concerning its reactivity, previous studies on degradation of **1** in aqueous media describe slow rearrangement or hydrolysis of the four membered ring.[14] Being a monocyclic β-lactam, **1** could in principle undergo photochemical ring splitting to give reactive intermediates, whereas it should react only sluggishly with nucleophiles win the dark. Moreover, the photoreactivity of **1** should increase in the presence of electron donors, such as the aromatic side chains of the Tyr or Trp units of HSA.[15] The obtained results indicate that **1** is indeed photolabile, giving rise to a reactive ketene intermediate that undergoes nucleophilic attack by Lys414 and Lys525, which are located in sub-domains IIIA and IIIB of HSA, respectively, leading to covalent adduct formation. In addition, the docking and MD simulation studies performed provide an insight into the molecular basis of the selectivity of **1** for these sub-domains of HSA and the covalent modification mechanism.

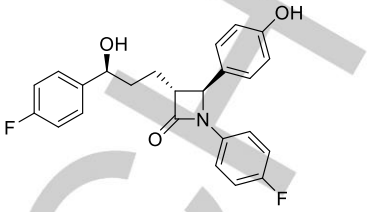

Chart 2. Chemical structure of ezetimibe **1**.

Results and Discussion

Photochemistry of 1 in the absence of protein. Due to the poor solubility of **1** in water, acetonitrile as well as a 9:1 (v/v) mixture of acetonitrile and water were employed as solvents. The results were similar, although the process was markedly faster at shorter wavelengths. Irradiation of **1** was performed at λ_{max} = 300 and 254 nm, in a multilamp photoreactor. The course of the reaction was followed by ^{1}H-NMR spectroscopy. After purification by column chromatography, imine **2**[16] and lactone **3**[17] were separated from the reaction crude as the sole photoproducts (Scheme 1). The ^{1}H- and ^{13}C-NMR spectra of isolated **2** matched with those of a commercially available sample, while in the case of **3**, they were compared with data reported in the literature.[17] The corresponding ^{1}H and ^{13}C-NMR spectra are shown in the SI (Figures S1-S4).

The reaction mechanism is outlined in Scheme 1. The anilide moiety would undergo N-CO bond splitting from the excited state; subsequent C-C bond cleavage of the primary biradical **I** would afford the corresponding retro-Staudinger products, namely **2** and ketene **II**; the latter was not even detected, since it rapidly evolves to the stable lactone **3**, through an intramolecular nucleophilic attack of the hydroxyl group to the ketene carbon.

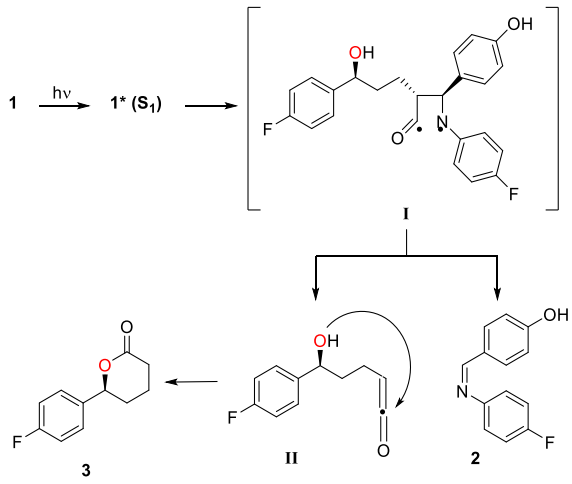

Scheme 1. Photoreactivity of **1** in acetonitrile.

To gain deeper insight into the excited states involved in the process, absorption, fluorescence and phosphorescence spectroscopy measurements were carried out on **1**. Thus, the absorption spectrum of **1** in MeCN (Figure S5 in SI) displayed a maximum at 285 nm and reached the UVB edge of the solar radiation. The fluorescence spectrum in the same solvent exhibited a maximum at 314 nm. From the intersection between the normalized emission (black trace, Figure 1) and excitation bands (red trace, Figure 1), a singlet energy of 97 kcal mol^{-1} was obtained. In the phosphorescence spectrum, recorded in EtOH at 77 K (blue trace, Figure 1), the maximum was located at 400 nm; the triplet energy obtained from this emission curve was 80 kcal mol^{-1}. Thus, since the reported value for bond dissociation energy of the N-CO bond is *ca.* 82 kcal mol^{-1},[18] thermodynamic requirements indicate that the initial N-CO bond cleavage should preferentially occur from the singlet excited state.

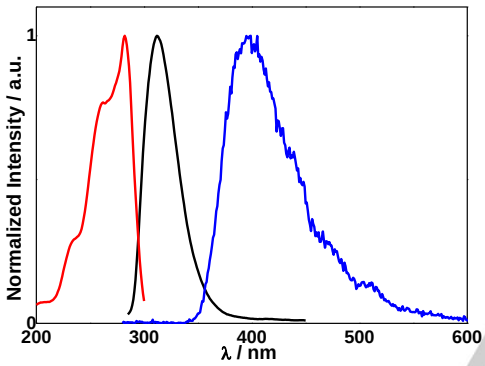

Figure 1. Normalized fluorescence emission (black trace) and excitation (red trace) spectra of **1** at 1 × 10^{-5} M concentration, in MeCN, at T = 295 K, under air; phosphorescence emission (blue trace) of **1** at 2 × 10^{-5} M concentration, in EtOH, at T = 77 K, under air.

Dark binding of 1 to HSA. Binding experiments were performed following an established methodology based on the displacement of site-specific fluorescent probes by non-emitting compounds, such as **1**. For this purpose, dansylamide (DA) and dansylglycine (DG) were taken as site I and site II markers, respectively.[19]

Selective excitation at 350 nm of DA/HSA or DG/HSA complexes gave rise to fluorescence emission centred at 480 or 475 nm, respectively. Figures S6 and S7 in the SI show the emission changes observed upon addition of ibuprofen (IBP, site II probe) or warfarin (WAR, site I probe) to the DG/HSA and DA/HSA systems. As expected for a site II ligand, addition of increasing amounts of IBP to the DG/HSA solution (at 1/1 molar ratio) induced a decrease of its emission intensity. Thus, DG was displaced out of the protein, and consequently a weaker and red-shifted emission was observed. In the case of DA/HSA, a similar behaviour was observed with WAR as displacer.

Experiments performed with **1** indicate that the drug possesses higher affinity towards site II. Although the binding constant value cannot be accurately determined due to the extremely low solubility of **1** in PBS, **1** clearly does not displace DG from site II, while IBU does. Interestingly, when DA is bound to site I, **1** binds free site II, which produces an allosteric effect that provokes a compression of site I and a parallel enhancement of DA fluorescence. Similar examples of allosteric effects can be found in the literature.[20] The trend is shown in Figure 2, a plot of I/I_0 *vs* equivalents of ligand added, constructed with data from the fluorescence experiments that appear in Figures S6 and S7 in the SI.

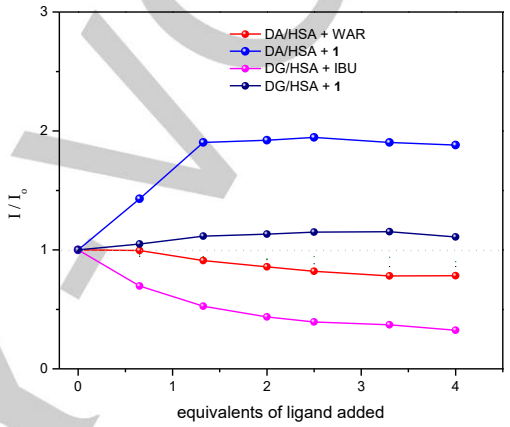

Figure 2. Variation of relative fluorescence intensity observed for probe-albumin solutions (4 × 10^{-5} M, 1:1 molar ratio) at λ_{em}= 480 nm for DA/HSA and 475 nm for DG/HSA, upon addition of WAR, IBU or **1**.

From the above experiments, it can be inferred that the value of the binding constant of **1** to site II is lower than that of IBU and DG (that are in the range of 2-3 ×10^6).[21] Indeed, it is probably one order of magnitude lower, since DG is not displaced even after addition of four equivalents of **1**. Concerning the stoichiometry of the complex, Job Plot experiments could not be performed, due to the poor solubility of **1** in PBS. However, it appears to be close to 1:1 (may be with some contribution from a 1:2 complex), since the fluorescence of DA in HSA increases until addition of *ca*. 1.3 equivalents of **1**, and then reaches a plateau.

Proteomic analysis of the photobinding of 1 to HSA. Formation of covalent photoadducts was investigated by proteomic analysis; these experiments would indicate precisely which (if any) amino acid(s) are covalently modified after irradiation of **1** in the presence of HSA. Thus, the photoreactivity of **1** within HSA was addressed by HPLC-nanoESI analysis. The procedure consisted on trypsin digestion to cleave peptide chains mainly at the carboxyl side of Lys or Arg residues (unless they are neighbour to a Pro residue), followed by HPLC-MS/MS. The process allowed obtaining information on the modified peptide sequence and characterizing the adduct. Full scan and fragmentation data files were analysed by using the Mascot® database search engine (Matrix Science, Boston, MA, USA) and by entering variable modifications that take into account the main

possible residues (Lys) able to react with ketene II obtained after cleavage of the β-lactam ring. Sequence coverage was 94%. The results are shown in Figure 3, with the modified peptides indicated in red.

The main result was identification of two adducts in $_{414}$KVPQVSTPTLVEVSR$_{428}$ and $_{525}$KQTALVELVQ$_{534}$ (Figure 3), with an increment of 194 amu. The modification site of the two peptide sequences was assessed by tandem mass experiments on the trypsin digests. The ESI-MS/MS spectra and fragmentation pattern are shown in Figures S8 and S9. The MS/MS analysis of fragment ions $_{414}$KVPQVSTPTLVEVSR$_{428}$ and $_{525}$KQTALVELVQ$_{534}$ showed that the modified amino acids are Lys414 and Lys525, respectively). Products resulting from transimination of imine **2** were not detected, even if they were specifically searched. However, their formation cannot be completely ruled out, since once formed, they would probably be hydrolysed under the trypsin digestion conditions. The lack of covalent binding of benzaldehyde to proteins when analysed in a similar manner has been described in a previous work.[22]

MKWVTFISLL FLFSSAYSRG VFRRDAHKSE VAHRFKDLGE ENFKALVLIA
FAQYLQQCPF EDHVKLVNEV TEFAKTCVAD ESAENCDKSL HTLFGDKLCT
VATLRETYGE MADCCAKQEP ERNECFLQHK DDNPNLPRLV RPEVDVMCTA
FHDNEETFLK KYLYEIARRH PYFYAPELLF FAKRYKAAFT ECCQAADKAA
CLLPKLDELR DEGKASSAKQ RLKCASLQKF GERAFKAWAV ARLSQRFPKA
EFAEVSKLVT DLTKVHTECC HGDLLECADD RADLAKYICE NQDSISSKLK
ECCEKPLLEK SHCIAEVEND EMPADLPSLA ADFVESKDVC KNYAEAKDVF
LGMFLYEYAR RHPDYSVVLL LRLAKTYETT LEKCCAAADP HECYAKVFDE
FKPLVEEPQN LIKQNCELFE QLGEYKFQNA LLVRYTKKVP QVSTPTLVEV
SRNLGKVGSK CCKHPEAKRM PCAEDYLSVV LNQLCVLHEK TPVSDRVTKC
CTESLVNRRP CFSALEVDET YVPKEFNAET FTFHADICTL SEKERQIKKQ
TALVELVKHK PKATKEQLKA VMDDFAAFVE KCCKADDKET CFAEEGKKLV
AASQAALGL

Figure 3. Amino acid sequence obtained after irradiation of HSA/**1** protein complex, with the non-matched amino acids in green. The modified peptides are in red, and the altered amino acid residues are yellow-highlighted.

Computational studies. Docking and MD simulations. The results of our proteomic studies revealed that irradiation of the HSA/**1** protein complex at 1:1 molar ratio causes the chemical modification in a similar proportion of Lys414 and Lys525, which are located in sub-domains IIIA and IIIB, respectively (Figure 4).

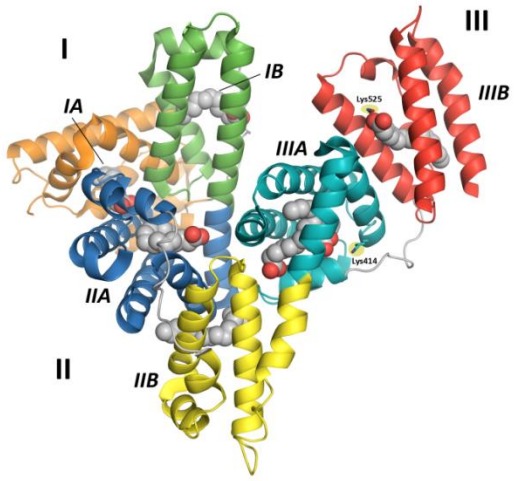

Figure 4. Crystal structure of HSA complexed with palmitic acid (PDB code 4BKE,[23] 2.35 Å). The three repeated domains I–III and each sub-domains A–B are highlighted with different colors and labeled. The complex contains seven palmitic acid molecules, depicted in spheres. The side chain of Lys525 and Lys414, which are located in sub-domains IIIB (red) and IIIA (cyan), respectively, are shown in sticks and labeled.

The structure of HSA consists in three homologous helical domains, namely I-III, each of which is divided into two sub-domains, A and B.[23] In addition, the experimentally observed additional mass of 194 of the lysine residues suggests that in both cases nucleophilic addition of their corresponding ε-amino groups to the generated ketene intermediate after UV irradiation takes place to afford the corresponding amide adducts (Figure 5).

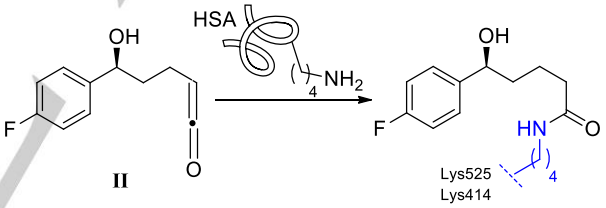

Figure 5. Protein adduct resulting after irradiation of the HSA/**1** protein complex.

In an effort to understand in atomic detail the covalent modification mechanism and to gain insight into the molecular basis selectivity for sub-domains IIIA and IIIB, molecular docking and MD simulation studies were carried out, which is described below. The binding modes of **1** in sub-domains IIIA and IIIB of HSA were first studied by molecular docking using the program GOLD[24] version 5.2 and the available enzyme coordinates of the crystallographically determined HSA in complex with palmitic acid (PDB code 4BKE,[25] 2.35 Å). This structure was chosen because palmitic acid, in addition to domains I and II, also binds in sub-domains IIIA and IIIB (Figure 4). The positions of the palmitic acid molecules in each of the identified sub-domains were used to define the recognition site and the radius was set to 10 Å. Docking studies were independently carried out in sub-domains IIIA and IIIB. Moreover, in order to assess the reliability of the postulated binding, MD simulation studies were then conducted with the highest score solutions obtained by docking for each sub-domain IIIA and IIIB. The monomer of the HSA-IIIA/**1** and HSA-IIIB/**1** protein complexes in a truncated octahedron of water molecules

obtained with the molecular mechanics force field AMBER[26] was employed. To get insight into the covalent addition mechanism, these simulation studies were carried out considering the two possible protonation states of Lys414 and Lys525. The results of these studies are discussed below.

*Binding of **1** and covalent addition to sub-domain IIIB* – The results from 100 ns dynamic simulation showed that the proposed binding for **1** in sub-domain IIIB obtained by docking was reliable as this complex proved to be stable during the simulation. Analysis of the root-mean-square deviation (rmsd) for the whole protein backbone (C_α, C, N and O atoms) calculated in the complex obtained from MD simulations studies revealed that it varies between 1.5–3.4 Å (average of 2.2 Å) and is relatively low for sub-domain IIIB (0.8–1.6 Å and an average of 1.2 Å) (Figure S10). These studies revealed that **1** would be anchored to sub-domain IIIB of HSA *via* four polar interactions involving the lactam carbonyl group and the two hydroxyl groups (Figure 6). Specifically, the ligand would establish: (a) an electrostatic interaction between its lactam carbonyl and the protonated ε-amino group of Lys525; (b) two hydrogen bonds between its secondary hydroxyl group and the main carbonyl group of Lys525 and the amide side chain of Asn405; and (c) a hydrogen bond between its phenol group and the carboxylate of Asp549.

Three main reasons led us to consider that Lys525 would be protonated in the HSA-IIIB/**1** complex: (1) the pKa of Lys525, calculated using the H^{++} Web server,[27] is 9.6; (2) comparison of the simulation studies with the two possible protonation states of Lys525 revealed that the ammonium group of the protonated Lys525 was located closer to the carbonyl group of **1** than the corresponding free amino group in the neutral Lys525; and (3) during the simulation, the protonated Lys525 establishes an electrostatic interaction with the carboxylate group of Glu518 (Figure S11A). The latter residue would be therefore well located to deprotonate Lys525 to afford the required nucleophile for the covalent modification reaction. Comparison of the position of the ligand during the simulation (Figures S12A–S12B) and the analysis of the variation of the relative distance between the atoms involved in the aforementioned polar interactions during the whole simulation revealed that the ligand is well fixed in this pocket and its conformation properly controlled by these residues (Figures S13A–S13C). In particular, the hydrogen bonding interaction between Lys525 and the secondary hydroxyl group in **1** is stable during ~89% of the simulation with an average distance of 2.8 Å. Moreover, the hydrogen bond of the phenol group of **1** with the carboxylate of Asp549 is observed during 76% of the simulation with an average distance of 2.7 Å. Another relevant interactions that contribute to the binding specificity of **1** to sub-domain IIIB would be the numerous apolar contacts within the pocket. Specifically, it would involve residues Phe507, Phe509, Ala528, Leu529, Leu532, Leu547, Phe551, Ala552, Leu547, and Met548 (Figure 6B).

In an effort to obtain further details of the covalent modification of Lys525 by **1**, the HSA/ketene protein complex and amide adduct were then explored by MD simulation studies. The results suggested that the capture of the ketene intermediate by nucleophilic attack of Lys525 must be very fast since this intermediate moves away quickly from the Lys525 vicinity. This was already observed during the minimization step, which is previous to the dynamic simulation. As shown in Figure 6C, the position of the resulting amide would be frozen by two hydrogen bonds involving the hydroxyl and NH groups of the amide adduct. In addition, the introduced chain in the ε-amino group of Lys525 would be embedded in the aforementioned apolar pocket.

*Binding of **1** and covalent addition to sub-domain IIIA* – Our computational studies showed that **1** would be fixed to sub-domain IIIA by three hydrogen bonds (Figures 6D and 6E). Two of them are direct strong contacts, one between the carbonyl group in **1** and the hydroxyl group of Ser489, and another one between the hydroxyl group in **1** and the main carbonyl group of Phe488. The analysis of the variation of the relative distance between the atoms involved in the aforementioned interactions revealed that they are very stable as they are present during ~89% of the simulation with an average distance of 2.8 Å (Figures S13D–S13E). The third hydrogen bond, which would be mediated by a water molecule, would involve the phenol group in **1** and the main carbonyl group of Val456 (Figure 6E). On the contrary to Lys525, Lys414 seems not to be contributing to the binding of **1**. Moreover, as for sub-domain IIIB, Lys414 would also be establishing an electrostatic interaction with Glu492 (Figure S11B) and **1** would have numerous aliphatic interactions with the apolar residues within the pocket. Specifically, residues Leu387, Ile388, Tyr411, Val415, Leu430, Val433, Leu453, Val456, Leu460, Val418 and Phe488 would be engaged.

As for sub-domain IIIB, the results from our MD simulations with the ketene intermediate suggested that this compound would also react rapidly with Lys414. Moreover, the resulting amide adduct would establish two hydrogen bonds involving the hydroxyl and the NH amide groups and the main carbonyl groups of Phe488 and Leu491, respectively (Figure 6F). In addition, the covalently modified Lys414 would be well embedded in the apolar pocket involving the aforementioned residues.

Remarkably, the analysis of the rmsd of the whole protein backbone for the HSA-IIIA/**1** complex revealed that it is significantly larger than for the HSA-IIIB/**1** one with values between 1.5–5.1 Å (average of 4.0 Å) (Figure S10). Although the rmsd values involving sub-domain IIIB are low (0.8–1.6 Å and an average of 1.2 Å), it seems that the HSA-IIIB/**1** complex would be more stable than the HSA-IIIA/**1** one. Comparison of the two protein complexes clearly reveals that when **1** binds to sub-domain IIIB it causes a large conformational change in this sub-domain of up to ~16 Å (Figure 7A). Similar findings were obtained for MD simulation studies carried out with the corresponding palmitic acid protein complexes (Figures 7B and 7C).

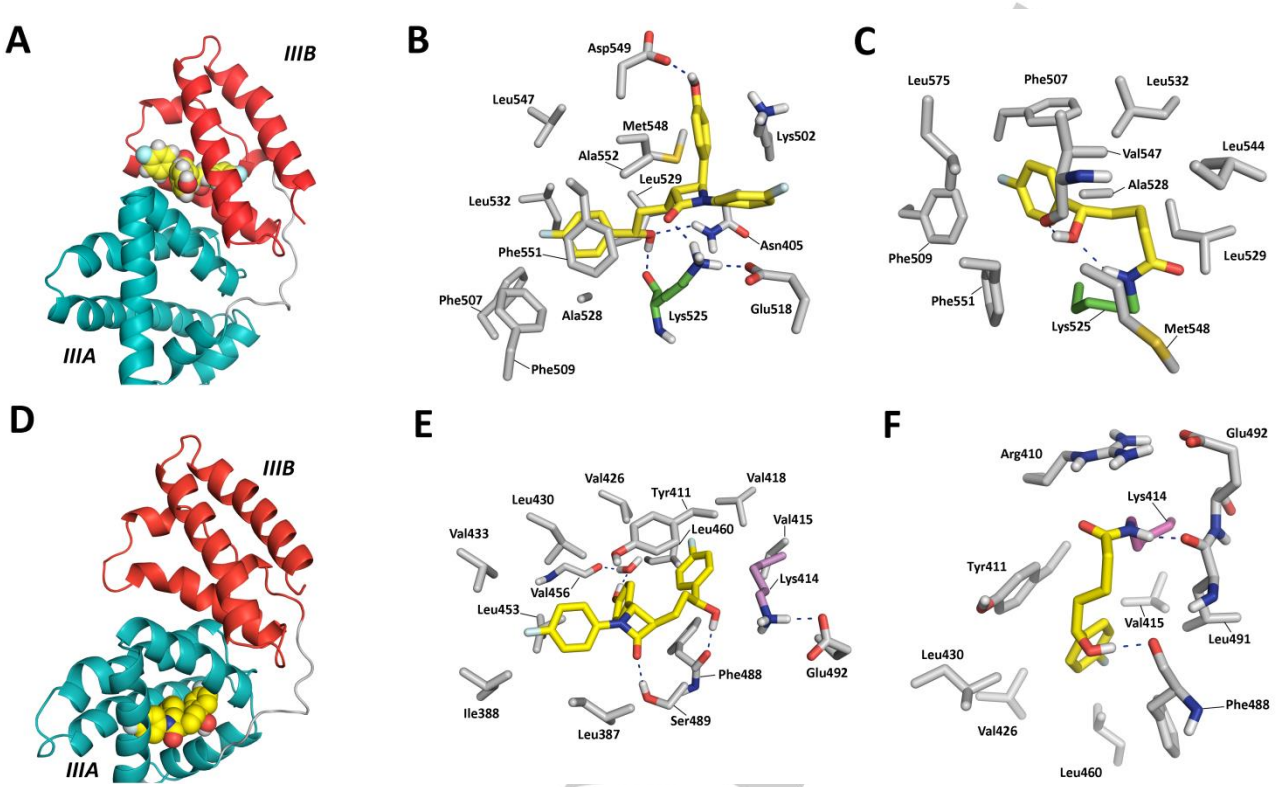

Figure 6. Proposed binding mode of **1** in sub-domains IIIB (A–C) and IIIA (D–E) obtained by docking and MD simulation studies. (A) Overall view of the HSA-IIIB/**1** complex. The main backbone of **1** is shown as yellow spheres while sub-domains IIIB and IIIA are highlighted in red and blue, respectively. (B) Interactions of **1** with sub-domain IIIB of HSA (gray). A snapshot after 80 ns is shown. (C) Detailed view of the HSA-IIIB/**1** adduct. The binding mode of the covalently modified Lys525 (green) through the formation of an amide bond (yellow) is shown. Snapshot taken after 80 ns. (D) Overall view of the HSA-IIIA/**1** complex. (E) Interactions of **1** with sub-domain IIIA of HSA. A snapshot after 100 ns is shown. (F) Detailed view of the HSA-IIIA/**1** adduct. The binding mode of the covalently modified Lys414 (violet) through the formation of an amide bond (yellow) is shown. Hydrogen bonding and electrostatic interactions between the ligand and HSA are shown as blue dashed lines. Relevant side chain residues are shown and labelled.

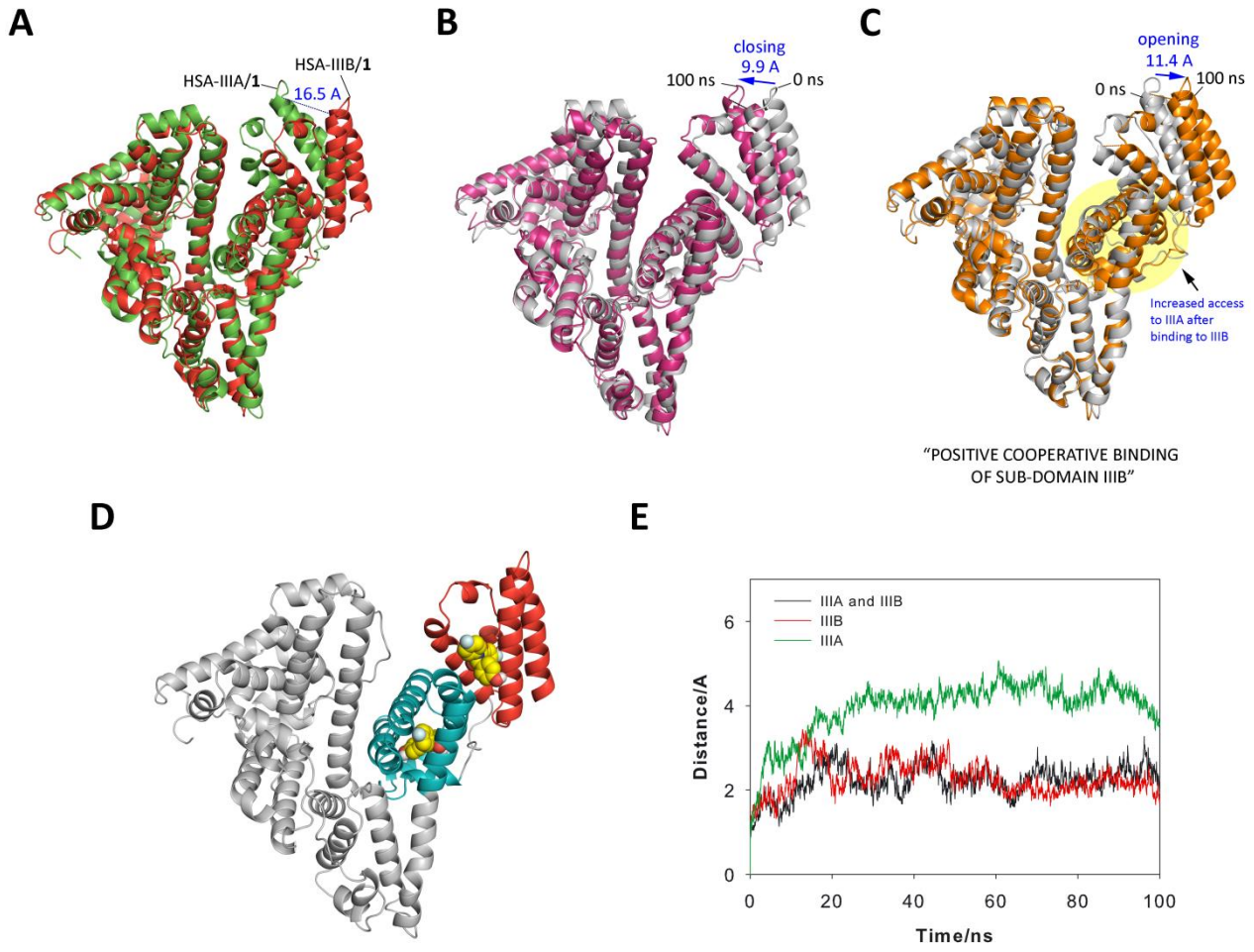

Figure 7. (A) Comparison of the HSA-IIIB/**1** (red) and HSA-IIIA/**1** (green) complexes. Ligands are not shown for clarity. Note the large conformational change that undergoes sub-domain IIIB when binding to **1**. (B) Comparison of the HSA-IIIA/palmitic acid binary complex after minimization and prior simulation (grey) and after 100 ns of dynamic simulation (pink). (C) Comparison of the HSA-IIIB/palmitic acid binary complex after minimization and prior simulation (grey) and after 100 ns of dynamic simulation (orange). Note how the binding of palmitic acid to sub-domain IIIB causes the opening of this sub-domain of up to 11.4 Å, whereas the binding to sub-domain IIIA yields the opposite effect. (D) Overall view of the proposed ternary HSA/**1** complex obtained by MD simulation studies. Sub-domains IIIA and IIIB are highlighted in blue and red, respectively, whereas the molecules of **1** are shown using yellow spheres. A snapshot after 60 ns is shown. (E) RMSD plots for the protein backbone (C^{α}, C, N, and O atoms) calculated in the three complexes [HSA-IIIA/**1** (green), HSA-IIIB/**1** (red) and HSA-IIIBA/**1**+**1** (black)] obtained from MD simulations studies.

Thus, when the ligand binds to sub-domain IIIB it causes a large opening of this protein region, whereas the binding to sub-domain IIIA leads to the opposite effect. This seems to be due to the interaction of the ligand in the interface between the two sub-domains (Figure 6A) that causes a remarkable increase of the protein volume in this region and a dramatic reduction of the flexibility of sub-domain IIIB. The relevant conformational changes that HSA can undergo on binding several ligands, specifically in domains I and III, was also previously reported by Curry *et al.*[27] Thus, comparison of the crystal structures of HSA/myristic acid protein complex (PDB code 1BJ5,[28] 2.5 Å) with the wild-type HSA (PDB code 1AO6,[29] 2.5 Å) proved to have a rmsd value after superposition of 479 α-carbon atoms of 2.90 Å (Figure S14). Therefore, taking into account: (i) the similar proportion obtained for the covalent modification of Lys414 and Lys525 in the proteomic studies, (ii) the greater accessibility of sub-domain IIIB than IIIA and (iii) the higher stability of the HSA-IIIB/**1** complex than the HSA-IIIA/**1** one, we considered that the formation of a ternary complex rather than a mixture of binary complexes would be reasonable; this is evaluated below.

*Ternary HSA/**1** complex.* Taking into account that: (i) depending on whether **1** binds to the sub-domain IIIA or IIIB conformationally different complexes may be formed, and (ii) in order to assess the affinity of **1** to sub-domain IIIA or IIIB, two possible pathways should be evaluated for the formation of the ternary complex (Scheme 2). Thus, we explored the incorporation of 1 to the free sub-domain IIIB in the HSA-IIIA/**1** protein complex to afford the HSA-IIIAB/**1**+**1** one (A) and the opposite situation to give complex B. The binding free energies of **1** in each sub-domain of complexes A and B were calculated using the MM/PBSA[30]

approach in explicit water (generalized Born, GB) as implemented in Amber (Table 1).

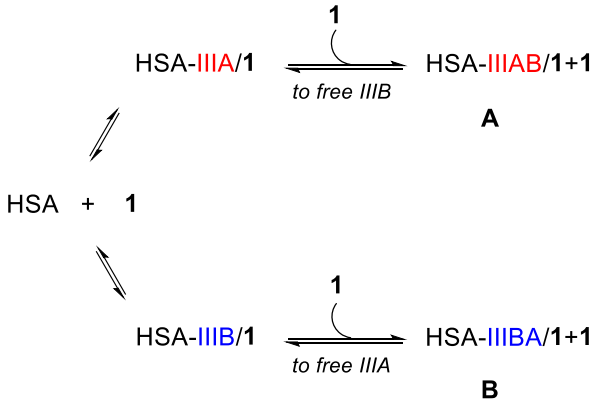

Scheme 2. Possible formation of the protein ternary complex.

Table 1. Calculated Binding Free Energies using MM/PBSA[a]

Ligand	Complex	Energy[b]
1	HSA-IIIA/**1**	−43.6 ± 0.2[c]
1	HSA-IIIB/**1**	−44.3 ± 0.2[c]
PAL[d]	HSA-IIIA/**PAL**	−43.9 ± 0.5[c]
PAL	HSA-IIIB/**PAL**	−50.2 ± 0.2[c]
1	HSA-IIIAB/**1+1** (**A**)	−43.9 ± 0.2[c] (sub-domain IIIA)
		−16.5 ± 0.2[c] (sub-domain IIIB)
1	HSA-IIIBA/**1+1** (**B**)	−41.0 ± 0.2[c] (sub-domain IIIA)
		−44.0 ± 0.2[c] (sub-domain IIIB)

[a]Energy units = kcal mol^{-1}; [b]only the last 80 ns of the whole simulation were considered for the calculations; [c]standard error of mean; [d]PAL = palmitic acid.

For the binary complexes, the results of our computational studies revealed that the affinity of **1**, as well as that of palmitic acid to sub-domain IIIB is higher than to IIIA. More importantly, the binding of a second **1** molecule to the free sub-domain IIIA of HSA-IIIB/**1** complex to afford complex B is 24.5 kcal more favorable than opposite case. In addition, our MD simulation studies also showed that the resulting complex is more stable than the HSA-IIIB/**1** one (Figures 7D and 7E). In fact, for the complex A, after 60 ns of dynamic simulation the ligand is no longer interacting with sub-domain IIIB. Therefore, it seems that the conformational changes that the protein undergoes as a result of the interaction of the ligand with sub-domain IIIB enhance the incorporation of a second ligand molecule to the more hidden pocket, sub-domain IIIA. Thus, HSA seems capable of transporting two **1** molecules in domain III due to a "positive cooperative binding" of sub-domain IIIB. This effect explains the unexpected and efficient experimentally observed covalent modification of Lys414, which is located in a highly hidden pocket of HSA.

Hence, once the ketene intermediate is generated by irradiation of the HSA/**1** protein complex, covalent attachment would probably occur by nucleophilic attack of Lys525 and Lys414, which would be triggered by Glu518 and Glu492, respectively, acting as the general base (Scheme S1). The MD simulation studies carried out with the HSA/ketene intermediate in both sub-domains suggest that the ketene reacts rapidly with both lysine residues.

Conclusions

The results obtained in the present work constitute an unambiguous proof supporting that, in addition to the known nucleophilic ring opening of β-lactams by the free amino group of lysine residues, there can be an alternative protein haptenation pathway by this family of drugs. It consists on the photochemical ring splitting of the β-lactam ring following a formal retro-Staudinger reaction, to give a highly reactive ketene intermediate that is attacked by the neighbouring lysines. In the case of ezetimibe, a β-lactam drug with anti-cholesterol activity, selective photobinding to Lys414 and Lys525 of HSA is demonstrated by proteomic analysis, in agreement with the expectations from docking and MD simulation studies. The latter studies also show that the specificity of ezetimibe for sub-domains IIIA and IIIB is due to the formation of several strong hydrogen bonding interactions with residues: (i) Phe488, Ser489 and Val456 (for sub-domain IIIA) and (ii) Asp549, Asn405 and Lys525 (sub-domain IIIB) as well as numerous lipophilic interactions with apolar residues within those pockets. The nucleophilic attack of Lys525 and Lys414 to the ketene intermediate would be triggered by Glu518 and Glu492, respectively, acting as the general base. These computational studies also reveal that the unexpected and efficient covalent modification of Lys414, which is located in a quite hidden pocket (sub-domain IIIA), would be possible due to a positive cooperative binding of sub-domain IIIB. Thus, the interaction of the ligand with sub-domain IIIB seems to cause a large opening of the protein that would enhance the binding of a second ligand molecule in this less accessible internal region. Work is currently in progress, to investigate the possible generality of the novel haptenation route in the widely employed penicillins and cephalosporins antibiotics.

Acknowledgements

Financial support from the Spanish Ministry of Economy and Competiveness (CTQ2013-47872-C2-1-P, CTQ2016-78875-P, SAF2013-42899-R, SAF2016-75638-R), Generalitat Valenciana (PROMETEOII/2013/005), the Xunta de Galicia (Centro singular de investigación de Galicia accreditation 2016-2019, ED431G/09) and the European Union (European Regional Development Fund -ERDF) is gratefully acknowledged. E. L. thanks the Xunta de Galicia for a postdoctoral fellowship. We are grateful to the Centro de Supercomputación de Galicia (CESGA) for use of the Finis Terrae II supercomputer. The proteomic analysis was performed in the proteomics facility of SCSIE University of Valencia that belongs to ProteoRed PRB2-ISCIII and is supported by grant PT13/0001, of the PE I+D+i 2013-2016, funded by ISCIII and FEDER.

Keywords: Ezetimibe • Human Serum Albumin • Molecular Dynamics Simulations • Photoallergy • Photobinding

[1] (a) M. G. P. Page, Ch 3, Beta-Lactam Antibiotics in *Antibiotic Discovery and Development*, (Eds. T. J. Dougherty, M. J. Pucci), Springer US, Boston, MA, **2011**, pp. 79–117; (b) B. Thakuria, K. Lahondefinite, *J. Clin. Diag. Res.* **2013**, *7*, 1207–1214; (c) T. P. Van Boeckel, S. Gandra, A. Ashok, Q. Caudron, B. T. Grenfell, S. A. Levin, R. Laxminarayan, *Lancet Infect. Dis.* **2014**, *14*, 742–750; (d) R. P. Elander, *Appl. Microbiol. Biotechnol*. **2003**, *61*, 385–392.

[2] (a) A. Ariza, C. Mayorga, T. D. Fernández, N. Barbero, A. Martín-Serrano, D. Pérez-Sala, F. J. Sánchez-Gómez, M. Blanca, M. J. Torres, M. I. Montañez, *J. Investig. Allergol. Clin. Immunol*. **2015**, *25*, 12–25; (b) R. Rodríguez-Pena, C. Antúnez, E. Martin, N. Blanca-López, C. Mayorga, M. J. Torres, *Expert Opin. Drug Saf.* **2006**, *5*, 31–48; (c) M. Blanca, A. Romano, M. J. Torres, J. Fernández, C. Mayorga, J. Rodríguez, P. Demoly, P. J. Bousquet, H. F. Merk, M. L. Sanz, H. Ott, M. Atanaskovic-Markovic, *Allergy* **2009**, *64*, 183–798.

[3] (a) R. Solensky, *J. Allergy Clin. Immunol.* **2014**, *133*, 797–798; (*b*) S. Bhattacharya, *J. Adv. Pharm. Technol. Res*. **2010**, *1*, 11–17.

[4] (a) A. Romano, C. Mayorga, M. J. Torres, M. C. Artesani, R. Suau, F. Sánchez, E. Pérez, A. Venuti, M. Blanca, *J. Allergy Clin. Immunol.* **2000**, *106*, 1177–1183; (b) W. A. Jr. Prescott, D. D. DePestel, J. J. Ellis, R. E. I. Rega, *Clin. Infect. Dis.* **2004**, *38*, 1102–1107; (c) M. J. Torres, A. Ariza, C. Mayorga, I. Dona, N. Blanca-López, C. Rondon, M. Blanca, *J. Allergy Clin. Immunol.* **2010**, *125*, 502–505.

[5] (a) M. Fernández-Rivas, C. Pérez Carral, M. Cuevas, C. Martí, A. Moral, C. J. Senent, *J Allergy Clin Immunol.* **1995**, *95*, 748–750; (b) K. H. Baggaley, K. H.; A. G. Brown, C. J. Schofield, *Nat. Prod. Rep.* **1997**, *14*, 309–333; (c) R. G. Edwards, J. M. Dewdney, R. J. Dobrzanski, D. Lee, *Int. Arch. Allergy Immunol*. **1988**, *85*, 184–189.

[6] (a) G. F. Gerberick, J. A. Troutman, L. M. Foertsch, J. D. Vassallo, M. Quijano, R. L. Dobson, C. Goebel, J. P. Lepoittevin, *Toxicol. Sci*. **2009**, *112*, 164–174; (b) S. F. Martin, P. R. Esser, S. Schmucker, L. Dietz, D. J. Naisbitt, B. K. Park, M. Vocanson, J. F. Nicolas, M. Keller, W. J. Pichler, M. Peiser, A. Luch, R. Wanner, E. Maggi, A. Cavani, T. Rustemeyer, A. Richter, H. J. Thierse, F. Sallusto, *Cell. Mol. Life Sci.* **2010**, *67*, 4171–4184; (c) I. Chipinda, J. M. Hettick, P. D. Siegel, *J. Allergy* **2011**, 839682; (d) B. Schnyder, W. Pichler, *Mayo Clin. Proc*. **2009**, *84*, 268–272; (e) J. T. DiPiro, N. F. Jr. Adkinson, R. G. Hamilton, *Antimicrob. Agents Chemother.* **1993**, *37*, 1463–1467.

[7] (a) D. J. Naisbitt, R. G. Nattrass, M. O. Ogese, *Immunol. Allergy Clin. N. Am*. **2014**, *34*, 691–705; (b) M. J. Torres, M. Blanca, J. Fernandez, A. Romano, A. Weck, W. Aberer, K. Brockow, W. J. Pichler, P. Demoly, *Allergy* **2003**, *58*, 961–972; (c) B. B. Levine, Z. Ovary, *J. Exp. Med.* **1961**, *114*, 875–905; (d) E. Pérez-Inestrosa, R. Suau, M. I. Montañez, R. Rodríguez, C. Mayorga, M. J. Torres, M. Blanca, *Curr. Opin. Allergy Clin. Immunol*. **2005**, *5*, 323–330; (e) F. Sánchez-Sancho, E. Pérez-Inestrosa, R. Suau, M. I. Montañez, C. Mayorga, M. J. Torres, A. Romano, M. Blanca, *J. Mol. Recognit.* **2003**, *16*, 148–;156; (f) F. Moreno, M. Blanca, C. Mayorga, S. Terrados, M. Moya, E. Pérez, R. Suau, J. M. Vega, J. García, A. Miranda, *et al. Int. Arch. Allergy Immunol*. **1995**, *108*, 74–81; (g) P. de Haan, A. J. de Jonge, T. Verbrugge, D. M. Boorsma, *Int. Arch. Allergy Appl. Immunol*. **1985**, *76*, 42–46; (h) C. Mayorga, T. Obispo, L. Jimeno, M. Blanca, J. Moscoso del Prado, J. Carreira, J. J. García, C. E. Juárez, *Toxicology* **1995**, *97*, 225–234.

[8] (a) X. Meng, R. E. Jenkins, N. G. Berry, J. L. Maggs, J. Farrell, C. S. Lane, A. V. Stachulski, N. S. French, D. J. Naisbitt, M. Pirmohamed, B. K. Park, *J. Pharmacol. Exp. Ther.* **2011**, *338*, 841–849; (b) F. R. Batchelor, J. M. Dewdney, D. Gazzard, *Nature* **1965**, *206*, 362–364.

[9] (a) A. Ariza, D. Garzón, D. R. Abanades, V. de los Ríos, G. Vistoli, M. J. Torres, M. Carini, G. Aldini, D. Pérez-Sala, *J. Proteomics* **2012**, *77*, 504–520; (b) M. Blanca, C. Mayorga, F. Sánchez, J. M. Vega, J. Fernández, C. Juárez, R. Suau, E. Pérez, *Allergy* **1991**, *46*, 632–638.

[10] P. S. Kelkar, J. T.-C. Li, *N. Engl. J. Med.* **2001**, *345*, 804–809.

[11] (a) M. Fasano, S. Curry, E. Terreno, M. Galliano, G. Fanali. P. Narciso, S. Notari, P. Ascenzi, *IUBMB Life* **2005**, *57*, 787–796 (b) J. Ghuman, P. A. Zunszain, I. Petitpas, A. A. Bhattacharya, M. Otagiri, S. J. Curry*, Mol. Biol.* **2005**, *353*, 38−52.

[12] D. Garzón, A. Ariza, L. Regazzoni, R. Clerici, A. Altomare, F. R. Sirtori, M. Carini, M. J. Torres, D. Pérez-Sala, G. Aldini, *Chem. Res. Toxicol*. **2014**, *27*, 1566–1574.

[13] T. Kosoglou, P. Statkevich, A. O. Johnson-Levonas, J. Paolini, A. J. Bergman, K. B. Alton, *Clin. Pharmacokinet.* **2005**, *44*, 467–494.

[14] (a) J. Batova, A. Imramovsky, J. Hajicek, L. Hejtmankova, J. Hanusek, *J. Pharm. Sci*. **2014**, *103*, 2240–2247; (b) J. Batova, A. Imramovsky, J. Hanusek, *J. Pharm. Biomed. Anal*. **2015**, *107*, 495–500.

[15] (a) M. Fischer, *Chem. Ber.* **1968**, *101*, 2669–2678; (b) H. Fabre, H. Ibork, D. A. Lerner, *J. Pharm. Sci.* **1994**, *83*, 553–558; (c) E. Rossi, G. Abbiati, E. Pini, *Tetrahedron* **1999**, *55*, 6961–6970; (d) R. Alcázar, P. Ramírez, R. Vicente, M. J. Mancheño, M. A. Sierra, M. Gómez-Gallego, *Heterocycles* **2001**, *55*, 511–521; (e) A. K. Mukerjee, A. K. Singh, *Synthesis* **1975**, 547–589; (f) A. K. Mukerjee, A. K. Singh, *Tetrahedron* **1978**, *34*, 1731–1767; (g) R. Pérez-Ruiz, J. A. Sáez, M. C. Jiménez, M. A. Miranda, *Org. Biomol. Chem*. **2014**, *12*, 8428–8432; (h) R. Pérez-Ruiz, J. A. Sáez, L. R. Domingo, M. C. Jiménez, M. A. Miranda, *Org. Biomol. Chem*. **2012**, *10*, 7928–7932.

[16] L. Jothi, G. Anuradha, G. Vasuki, R. R. Babu, K. Ramamurthi, *Acta Crystal. E* **2014**, *70*, o860.

[17] L. Zhou, X. Liu, J. Ji, Y. Zhang, W. Wu, Y. Liu, L. Lin, X. Feng, *Org. Lett*. **2014**, *16*, 3938–3941.

[18] (a) M. L. Andersen, *Acta Chem. Scand.* **1996**, *50*, 1045–1049; (b) S. G. Lias, J. E. Bartmess, J. G. Liebman, J. L. Holmes, R. D. Levin, W. G. Mayard, *J. Phys Chem. Ref. Data* **1988**, *17*, Suppl 1, 1-861.

[19] (a) V. S. Jisha, K. T. Arun, M. Hariharan, D. Ramaiah, *J. Am. Chem. Soc.* **2006**, *128*, 6024–6025. (b) L. H. Lucas, K. E. Price, C. K. Larive, *J. Am. Chem. Soc.* **2004**, *126*, 14258–14266.

[20] (a) D. E. Epps, T. J. Raub, F. J. Kezdy, *Anal. Biochem*. **1995**, *227*, 342–350; (b) M. Marin, V. Lhiaubet-Vallet, M. A. Miranda, *J. Phys. Chem. B* **2011**, 115, 2910–2915.

[21] (a) Z. M. Li, C. W. Wei, Y. Zhang, D. S. Wang, Y. N. Liu, *J Chromatogr B Analyt Technol Biomed Life Sci.* **2011**, 1934–1938.

[22] M. Aleksic, C. K. Pease, D. A. Basketter, M. Panico, H. R. Morris, A. Dell, *Toxicol. Vitro* **2007**, *21*, 723–733.

[23] J. Ghuman, P. A. Zunszain, I. Petitpas, A. A. Bhattacharya, M. Otagiri, S. Curry, *J. Mol. Biol.* **2005**, *353*, 38–52.

[24] http://www.ccdc.cam.ac.uk/solutions/csd-discovery/components/gold/

[25] A. Sivertsen, J. Isaksson, H. S. Leiros, J. Svenson, J. Svendsen, B. O. Brandsdal, *BMC Struct. Biol.* **2014**, *14*, 4.

[26] D. A. Case, J. T. Berryman, R. M. Betz, D. S. Cerutti, T. E. Cheatham III, T. A. Darden, R. E. Duke, T. J. Giese, H. Gohlke, A. W. Goetz, N. Homeyer, S. Izadi, P. Janowski, J. Kaus, A. Kovalenko, T. S. Lee, S. LeGrand, P. Li, T. Luchko, R. Luo, B. Madej, K. M. Merz, G. Monard, P. Needham, H. Nguyen, H. T. Nguyen, I. Omelyan, A. Onufriev, D. R. Roe, A. Roitberg, R. Salomon-Ferrer, C. L. Simmerling, W. Smith, J. Swails, R. C. Walker, J. Wang, R. M. Wolf, X. Wu, D. M. York, P. A. Kollman, AMBER 2015, University of California, San Francisco, **2015**.

[27] (*a*) J. C. Gordon, J. B. Myers, T. Folta, V. Shoja, L. S. Heath, A. Onufriev, *Nucleic Acids Res.* **2005**, *33* (Web Server issue):W368. (*b*) http://biophysics.cs.vt.edu/H++.

[28] S. Curry, H. Mandelkow, P. Brick, N. Franks, *Nature Struct. Biol.* **1998**, *5*, 827–835.

[29] S. Sugio, A. Kashima, S. Mochizuki, M. Noda, K. Kobayashi, *Protein Eng.* **1999**, *12*, 439–446.

[30] B. R. Miller III, T. D. McGee Jr., J. M. Swails, N. Homeyer, H. Gohlke, A. E. Roitberg, *J. Chem. Theory Comput.* **2012**, *8*, 3314–3321.

FULL PAPER

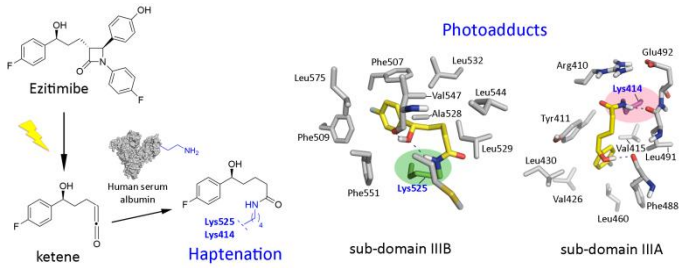

Raúl Pérez-Ruiz, Emilio Lence, Inmaculada Andreu, Daniel Limones-Herrero, Concepción González-Bello, Miguel A. Miranda and M. Consuelo Jiménez**

Page No. – Page No.

A Novel Pathway of Protein Haptenation by β-Lactams

A new haptenation mechanism of β-lactams drugs, which constitute the key step in the sequence of events leading to photoallergy, has been identified. Selecting human serum albumin as target protein and ezetimibe as probe, the covalent modification of Lys414 and Lys525 residues (located in sub-domains IIIA and IIIB) were identified. The process involves the photochemical ring splitting of the β-lactam ring of ezetimibe giving a highly reactive ketene intermediate that is trapped by the neighbouring lysine residues.